Experimental Correlation between the Flow and Magnus Characteristics of a Spinning Ogive-Nose Cylinder

JAMES M. MARTIN*
U.S. Army Air Mobility R & D Laboratory, Moffett Field, Calif.
AND
CHARLES W. INGRAM†
University of Notre Dame, Notre Dame, Ind.

Theme

AN experimental investigation of the Magnus force on a seven-caliber, tangent-ogive nosed cylinder is presented. Correlations between strain gage measurements of the Magnus force coefficient, smoke flow photographs and hot-wire surveys of the lee-side vortex region yield a flow model which explains a change in sign of the Magnus force coefficient with angle of attack. Of particular interest is the discovery that a Magnus effect can be due to a combined interaction between the boundary layer and lee-side vortices.

Contents

The objective of this Synoptic is to record the Magnus force on a seven-caliber, tangent-ogive nosed cylinder and then experimentally determine the flow phenomena which caused that force.

The Magnus force is known to be a function of Reynolds number Re, angle of attack α, and $Pd/2V_\infty$, where P = roll rate in rad/sec, d = diameter of the body in feet, and V_∞ = freestream velocity in fps. Thus, strain gage measurements of C_Y, side force coefficient, were taken for a Re/ft range from 2.55×10^5 to 5.75×10^5, an angle-of-attack range from 0° to 15° and a $Pd/2V_\infty$ range from 0.25 to 0.5 (Ref. 1). Since the same results occurred at each of the Reynolds numbers, only one representative Re is presented here to illustrate the Magnus phenomena.

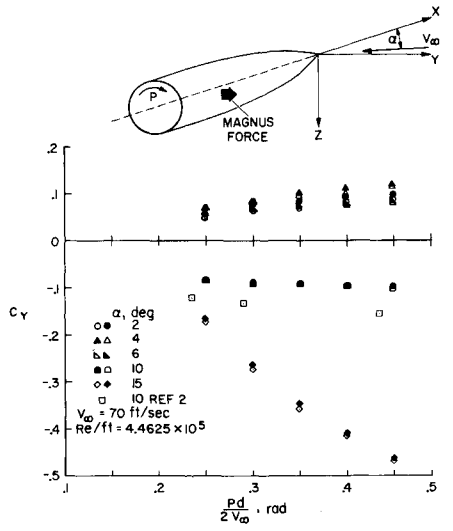

Fig. 1 C_Y **vs** $Pd/2V_\infty$ **for a varying roll rate and constant velocity.**

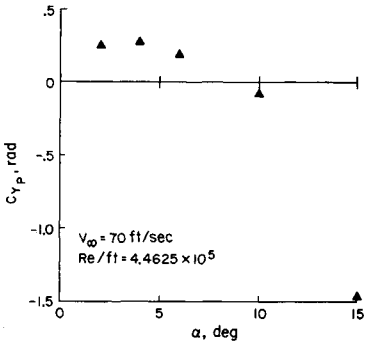

Fig. 2 C_{Y_p} **vs** α **at a constant velocity.**

Figure 1 depicts the force coordinate system used throughout this paper. This axis system is attached to the body but does not roll with it. Figure 1 also presents C_Y vs α for Re/ft = 4.46×10^5 (V_∞ = 70 fps). Two tests are shown at each α. Good repeatability is seen in these data as well as good agreement with C_Y data obtained from internal strain gage measurements on a similar model for approximately the same Re and $Pd/2V_\infty$ range. The C_Y data are approximately linear in $Pd/2V_\infty$; hence a straight line was fitted to the data using the method of least squares. The slopes from these fits yielded C_{Y_p}, Magnus force coefficient, which is plotted as a function of angle of attack in Fig. 2. These data show that C_{Y_p} is nonlinear in α with positive values at low angles of attack and negative values at high angles of attack.

To obtain a better knowledge of the Magnus force and its associated flowfield, smoke flow photographs of the lee-side vortex region were taken for the same test conditions as the strain gage measurements; Re/ft = 4.46×10^5, p = 0 to 2000 rpm, α = 0° to 15°. The results of the smoke flow tests are sketched in Fig. 3, and all references to the right (advancing side) or left (retreating side) of the test configuration are made viewing the model from the rear.

For α = 0° no lee-side vortices were seen to form and the wake region appeared to be symmetrical at all roll rates, thus indicating zero Magnus. At α = 2°, small vortices were seen to form at p = 0. However, no definite flowfield alterations were observed. Discrete lee-side vortices were again seen for p = 0 and α = 4°. As p increased to 1000 rpm both vortices were absorbed by the boundary layer and rotated in the direction of p. As the roll rate approached 1400 rpm, the vortices had become an integrated part of the boundary layer and a definite "hump" was present on the advancing side of the body as opposed to a minimal thickness on the retreating side, Fig. 3a. This distortion of the boundary layer rotated around the body with increased spin.

Received August 4, 1972; synoptic received January 30, 1973; revision received March 12, 1973. Full paper available from National Technical Information Service, Springfield, Va., 22151, as N73-18286 at the standard price (available upon request). Submitted by J. M. Martin to the Graduate School of the University of Notre Dame in partial fulfillment of the requirements for the Degree of Doctor of Philosophy.

Index categories: Rocket Vehicle Aerodynamics; LV/M Dynamics, Uncontrolled.

* Research Scientist, formerly Graduate Teaching Assistant, University of Notre Dame. Associate Member AIAA.

† Assistant Professor. Member AIAA.

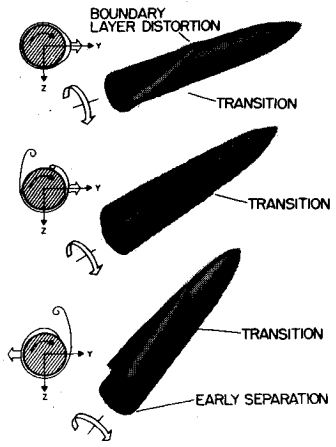

Fig. 3 Distortion of lee-side vortex region due to spin at low, medium, and high angles of attack.

For $\alpha = 6°$, $p = 0$ discrete lee-side vortices again formed. However, as the model was spun up the vortices retained their identity longer than at $\alpha = 4°$. As p increased from 1200 through 1800 rpm's the left vortex appeared very smooth and distinct while the right vortex was rough and hard to distinguish. Thus, it seemed that the left vortex was well formed and separated much farther forward than the right vortex as indicated in Fig. 3b.

For $\alpha = 15°$ discrete lee-side vortices appeared at $p = 0$. As the roll rate increased to 2000 rpm, the left vortex was pulled into the boundary layer while the right vortex maintained its identity (Fig. 3c).

Boundary-layer thickness measurements were made on both sides of the test model using a hot-wire anemometer to determine the existence of the flowfields described in Fig. 3. The boundary layer thickness δ was measured along the y-axis for the test range $\alpha = 0°$ to 15°, $Re/\text{ft} = 4.45 \times 0.10^5$, $p = 1800$ rpm. Table 1 presents δ on each side of the model as a function of angle of attack, for the probe positioned 3 in. forward of the model base. These data indicate that the boundary is thicker on the right side of the model than the left. Also, it is interesting that the boundary-layer thickness on the left side does not change for $\alpha = 0°$, 2°, and 4°, and then reduces by 0.0032 ft for $\alpha = 6°$. This indicates that the vortices have no effect on the retreating side boundary layer due to their low energy at small α's but could have an effect at $\alpha = 6°$. At $\alpha = 15°$, the boundary-layer thickness on the retreating side of the model is exactly half that produced at $\alpha = 0°$. The boundary-layer thickness is much smaller because of the high energy of the vortices.

The presence of a hump in the boundary layer at low angle of attack was more convincingly documented by placing the hot-wire at a constant Y position on each side of the test configuration 3 in. forward of the model base. The model was then allowed to spin down from $p = 2000$ rpm. The tests were performed for the same α range and Re/ft as the previous tests. The hot-wire again indicated that no hump was present on the left side of the model. However, when the hot-wire was placed on the right or advancing side of the model a hump or large mass of turbulent air passed by the hot-wire for $\alpha = 2°$, $p = 800$ rpm and $\alpha = 4°$, $p = 1400$ rpm. At $\alpha = 6°$ and 15° the boundary-layer thickness decreased as p decreased but no distinct hump passed the hot-wire. These results reaffirm the presence of a distortion due to spin in the boundary layer at low angles of attack.

The preceding strain gage, smoke flow and hot-wire anemometer investigations of the Magnus force and its associated flow characteristics of an ogive cylinder suggest that three flow regimes exist, causing the change in sign of the Magnus force with angle of attack. The first occurs at small angles of attack due to the low energy of the lee-side vortices; the second occurs at $\alpha = 6°$ where the left vortex is distinct; the third occurs at large angles of attack where the right vortex is distinct (Fig. 3).

At $\alpha = 2°$ and 4° the hot-wire and smoke flow results show that the two lee-side vortices are rotated to the advancing side of the body. If they were separated from the body, they would produce a high pressure on the advancing side and thus a negative Magnus force. However, since the strain gage results show a positive Magnus force, the lee-side vortices are absorbed into the boundary layer producing a hump or distortion which rotates in the direction of spin as the roll rate increases. It is hypothesized that the distorted boundary layer can be considered as an addition to the surface of the body. That is, if p is held constant, the distorted boundary layer can be added to the body thus producing a new body shape with $p = 0$. This new body with the hump on its right side has an increased cross flow velocity and a decreased pressure on that side. The higher pressure on the left side of the body produces a positive Magnus force which is consistent with the strain gage measurements. Martin[3] analytically predicted a negative Magnus force using a boundary-layer distortion approach. However, he produced his analytical Magnus prediction by assuming a laminar, incompressible, supersonic flow with very low spin rates. These assumptions appear to be valid in the supersonic flow case but are not valid here. Also, most available Magnus data do not show a positive trend at small angles of attack. This can be attributed to the fact that most available Magnus data are produced at more than three times the tunnel velocity shown here. This additional free-stream velocity can add to the energy of the lee-side vortices and decrease the boundary-layer effects.

Table 1 Boundary-layer thicknesses measured with a hot-wire anemometer

α	δ (left), ft	δ (right), ft
0	0.0312	0.0312
2	0.0312	0.0312
4	0.0312	0.0416
6	0.0286	0.0494
15	0.0182	0.0312

For $\alpha = 6°$ the left vortex appears to separate farther forward than the right vortex and maintains its identity throughout the range of $Pd/2V_\infty$ tested. This early separation on the left side of the body provides for a low local velocity and high pressure on the retreating side as opposed to a low pressure on the advancing side. This analysis is presented in Refs. 4 and 5 and describes the positive Magnus force seen in the strain gage data at $\alpha = 6°$.

For large angles of attack the lee-side vortices have sufficient energy to resist total absorption by the boundary layer. The separation line of the left vortex rotates in the direction of spin and the vortex itself is absorbed into the boundary layer as $Pd/2V_\infty$ increases, with the right vortex having enough energy to maintain its identity. The separation line of the right vortex produces a low local velocity and high pressure on the right side of the model, yielding a negative Magnus force as measured by the strain gage.

This analysis indicates that the Magnus effect on spinning symmetrical bodies is a complex interaction between the boundary layer and body vortices. The strain gage measurements combined with the smoke flow photographs and hot-wire analysis provide a unique experimental correlation which has furnished an insight into the nature of the Magnus and flow characteristics of spinning bodies.

References

[1] Martin, J. M., "A Correlation between the Flow and Magnus Characteristics of a Spinning Ogive-Noise Cylinder," Ph.D. dissertation, Aug. 1971, Univ. of Notre Dame, Notre Dame, Ind.

[2] Wood, S. R. and Lovelady, E. J., "Experimental Investigation of the Subsonic Magnus Characteristics of Aerodynamically Neutral Spin Stabilized Rocket Configurations," Rept. 2286, Oct. 1969, Emerson Electronics, St. Louis, Mo.

[3] Martin, J. C., "On Magnus Effects Caused by the Boundary Layer Displacement Thickness on Bodies of Revolution at Small Angles of Attack," Rept. 870 (Revised), June 1955, Ballistics Research Lab., Aberdeen Proving Ground, Md.

[4] Brown, F. N. M., *See the Wind Blow*, 636 Ostemo Place, South Bend, Indiana, 1971.

[5] Krahn, E., "Negative Magnus Force," *IAS Journal*, Vol. 25, April 1956, pp. 377–379.